# CP violation in decays into states with neutral kaons

Yuval Grossman,<sup>1,\*</sup> Paolo Leo,<sup>2,†</sup> Alberto Martini,<sup>2,‡</sup> Guglielmo Papiri,<sup>1,§</sup> and Armine Rostomyan<sup>2,¶</sup>

<sup>1</sup>Department of Physics, LEPP, Cornell University, Ithaca, NY 14853, USA

<sup>2</sup>Deutsches Elektronen-Synchrotron, 22607 Hamburg, Germany

(Dated: September 10, 2025)

# Abstract

CP violation in the kaon system can manifest itself in decays to final states containing neutral kaons. The effect is governed by an efficiency function that reflects the specific experimental setup. We demonstrate that this efficiency function factorizes into two components: the kaon energy spectrum and a universal detector-dependent factor. We show that matter effects on kaon oscillations can have a significant effect on CP asymmetries. We provide estimates of the theoretical prediction for some such CP asymmetries for a Belle II–type experiment.

<sup>\*</sup> yg73@cornell.edu

<sup>†</sup> paolo.leo@desy.de

<sup>&</sup>lt;sup>‡</sup> alberto.martini@desv.de

<sup>§</sup> gp343@cornell.edu

<sup>¶</sup> armine.rostomyan@desy.de

#### I. INTRODUCTION

In the standard model (SM), the CP asymmetry in the  $\tau$  decay

$$A_1 = \frac{\Gamma(\tau^+ \to \pi^+ K_S \overline{\nu_\tau}) - \Gamma(\tau^- \to \pi^- K_S \nu_\tau)}{\Gamma(\tau^+ \to \pi^+ K_S \overline{\nu_\tau}) + \Gamma(\tau^- \to \pi^- K_S \nu_\tau)}, \tag{1}$$

arises because  $\tau^+$  and  $\tau^-$  decay to different kaon interaction eigenstates  $(K^0 \text{ and } \overline{K}^0)$ , which project differently onto the mass eigenstates  $(K_S \text{ and } K_L)$ . The first theoretical estimate for the CP asymmetry  $A_1$  was given in Ref. [1],

$$A_1 \approx 2 \text{Re}[\epsilon] \approx 3.3 \times 10^{-3} \,,$$
 (2)

where  $\epsilon$  is the CP violation parameter measured in neutral kaon mixing. This result was derived assuming that the final state is a  $K_S$  eigenstate. It is important to note that experimentally the  $K_S$  in the final state is defined as the  $\pi\pi$  system with invariant mass  $m_{\pi\pi} \approx m_K$ . Later, in [2], this prediction was revisited showing that the fact that a  $K_S$  is identified by its decay to two pions introduces important effects due to  $K_L - K_S$  interference. As a result,  $A_1$  depends on the decay time of the kaon and the experimental requirements.

The CP asymmetry  $A_1$  has been investigated by the BaBar [3] and Belle [4] collaborations. The BaBar decay-rate asymmetry result shows a  $3\sigma$  tension with the SM prediction, while Belle's angular analysis finds results consistent with zero within  $O(10^{-2})$  per  $K_S$  mass bin.

The Belle II collaboration [5] aims to improve the measurement precision. However, the observed asymmetry in  $e^+e^- \to \tau^+\tau^-$  events includes background contributions from other  $\tau$  decays, particularly those involving two kaons,  $\tau^{\pm} \to K^{\pm}K_S\nu_{\tau}$  and  $\tau^{\pm} \to \pi^{\pm}K_SK_L\nu_{\tau}$ , with corresponding asymmetries defined as:

$$A_2 = \frac{\Gamma(\tau^+ \to \overline{\nu_\tau} K^+ K_S) - \Gamma(\tau^- \to \nu_\tau K^- K_S)}{\Gamma(\tau^+ \to \overline{\nu_\tau} K^+ K_S) + \Gamma(\tau^- \to \nu_\tau K^- K_S)}, \tag{3}$$

and

$$A_3 = \frac{\Gamma(\tau^+ \to \overline{\nu_\tau} K_L K_S \pi^+) - \Gamma(\tau^- \to \nu_\tau K_L K_S \pi^-)}{\Gamma(\tau^+ \to \overline{\nu_\tau} K_L K_S \pi^+) + \Gamma(\tau^- \to \nu_\tau K_L K_S \pi^-)} . \tag{4}$$

For an ideal experiment we expect  $A_1 = -A_2$  and  $A_3 = 0$ . However, as pointed out in Ref. [2], in general the experimentally measured CP asymmetries depend on an efficiency function, describing the probability to reconstruct a  $K \to \pi\pi$  decay as a function of the kaon rest-frame decay time, t. Thus, these equalities are violated in a real experiment. Ref. [2]

treated the efficiency function as universal across decay modes. However, it depends on the specific process from which the kaon originates.

In this work, we extend that analysis by showing that the reconstruction efficiency function factorizes into two fundamental parts: a universal, detector-specific efficiency in the laboratory frame, and process-dependent kaon energy spectrum. Moreover, we show that matter effects on neutral kaon oscillations can give very important corrections to the measured CP asymmetries. We provide theoretical predictions for all these asymmetries in the case of a Belle II-type experiment. We show that, given the anticipated precision at Belle II, it is safe to assume  $A_3 = 0$  and  $A_1 = -A_2$ , since the associated uncertainties are negligible compared to other sources of uncertainty. In contrast, corrections arising from the matter effects are subject to significant theoretical uncertainties and therefore should be studied within the experimental analysis.

#### II. THE EXPERIMENTAL ASYMMETRY

In general, the experimentally measured CP asymmetry  $A_{Exp,P}$  associated with a given  $\tau$  decay process P receives contributions from three distinct sources:

- 1. The intrinsic (direct) CP asymmetry in the  $\tau$  decay, denoted  $A_{Exp,P}^{\tau}$ ;
- 2. The contribution from CP violation in the kaon system, arising from neutral-kaon oscillations in the final state, denoted  $A_{Exp,P}^K$ ;
- 3. The detector-induced asymmetry,  $A_{Exp,P}^{\text{det}}$ , originating from possible differences in the detection efficiencies of the final-state particles in  $\tau^+$  versus  $\tau^-$  decays.

The first two contributions are genuine CP-violating effects, while the last term represents an artificial asymmetry induced by the detector. Assuming that all contributions are small, they can be treated additively:

$$A_{Exp,P} = A_{Exp,P}^{\tau} + A_{Exp,P}^{K} + A_{Exp,P}^{\det} . {5}$$

Within the SM, the first contribution,  $A_{Exp,P}^{\tau}$ , is negligible. Accordingly, in the following discussion we set  $A_{Exp,P}^{\tau} = 0$ . This work focuses on the second and third contributions to the asymmetry, which are related to the experimental reconstruction efficiency for detecting the kaons.

#### A. The kaon frame efficiency

We define f(t) to be the experimental reconstruction efficiency function for the detection of a neutral kaon in the final state of the  $\tau$  decay. Here t is the kaon decay time in the kaon rest frame. In general, f(t) carries 3 indices: the process P from which the kaon originated, P = 1, 2, 3 (related to the asymmetries in Eqs. (1), (3) and (4)); the charge of the  $\tau$ ; and the strangeness of the kaon, that is,  $K^0$  or  $\overline{K}^0$ . Thus, in general, for any process P there are four  $f_P(t)$  functions:

$$f_P^{+,K}, \qquad f_P^{+,\overline{K}}, \qquad f_P^{-,K}, \qquad f_P^{-,\overline{K}}.$$
 (6)

If the process P has only one neutral kaon in final state, as for  $A_1$  and  $A_2$ , then two of the above functions are irrelevant. Indeed, the decay processes written in terms of kaons interaction eigenstates are:

$$A_1: \quad \tau^+ \to \overline{\nu}\pi^+ K^0 \ , \tag{7}$$

$$A_2: \quad \tau^+ \to \overline{\nu} K^+ \overline{K}^0 \ , \tag{8}$$

meaning that we do not need to consider  $f_1^{-,K}$ ,  $f_1^{+,\overline{K}}$ ,  $f_2^{+,K}$ , and  $f_2^{-,\overline{K}}$ . For decays with two neutral kaons in final states, as in the case of  $A_3$ , all four combinations are relevant.

We further define

$$f_P^K(t) = \frac{f_P^{+,K}(t) + f_P^{-,\overline{K}}(t)}{2}, \qquad \Delta f_P^K(t) = \frac{f_P^{+,K}(t) - f_P^{-,\overline{K}}(t)}{2}, \tag{9}$$

$$f_P^{\overline{K}}(t) = \frac{f_P^{+,\overline{K}}(t) + f_P^{-,K}(t)}{2}, \qquad \Delta f_P^{\overline{K}}(t) = \frac{f_P^{+,\overline{K}}(t) - f_P^{-,K}(t)}{2},$$
 (10)

and the functions with no superindex

$$f_P(t) = f_P^K(t) + f_P^{\overline{K}}(t), \qquad \Delta f_P(t) = f_P^K(t) - f_P^{\overline{K}}(t) . \tag{11}$$

For the case of  $A_1$  we can make the kaon index implicit

$$f_1^K(t) = f_1(t) , \qquad f_1^{\overline{K}}(t) = 0 ,$$
 (12)

and similarly for  $A_2$ 

$$f_2^{\overline{K}}(t) = f_2(t) , \qquad f_2^{K}(t) = 0 ,$$
 (13)

where we have set  $f_1^{\overline{K}}$  and  $f_2^K$  to zero, as they are irrelevant for the relative processes. In the case of  $A_3$ , as we discuss in Section IV, both  $f_3^K$  and  $f_3^{\overline{K}}$  are relevant.

#### B. CP asymmetry for decays with one neutral kaon

We start by considering the CP asymmetry for a process P with a single neutral kaon in the final state. For the sake of simplicity we develop the formalism for  $A_1$ .

Under the assumptions stated above, the measured asymmetry is given by

$$A_{Exp,1} = \frac{\int_0^\infty dt \ [f_1^{+,K}(t)\Gamma_{\pi\pi}(t) - f_1^{-,\overline{K}}(t)\overline{\Gamma}_{\pi\pi}(t)]}{\int_0^\infty dt \ [f_1^{+,K}(t)\Gamma_{\pi\pi}(t) + f_1^{-,\overline{K}}(t)\overline{\Gamma}_{\pi\pi}(t)]} \ . \tag{14}$$

The rates,

$$\Gamma_{\pi\pi}(t) = \Gamma(K^0(t) \to 2\pi), \qquad \overline{\Gamma}_{\pi\pi}(t) = \Gamma(\overline{K}^0(t) \to 2\pi),$$
 (15)

are defined as the decay rates for  $K^0$  and  $\overline{K}^0$  into two pions, as a function of the decay time t in the reference frame of the kaon. These rates are known and are expressed in terms of measured physical parameters, see Eq. (32) and Eq. (33). We define

$$\Sigma_{\pi\pi}(t) = \Gamma_{\pi\pi}(t) + \overline{\Gamma}_{\pi\pi}(t), \qquad \Delta_{\pi\pi}(t) = \Gamma_{\pi\pi}(t) - \overline{\Gamma}_{\pi\pi}(t).$$
 (16)

We know experimentally that  $\Delta_{\pi\pi}(t)/\Sigma_{\pi\pi}(t) = O(\epsilon)$ . In addition, in all available experiments  $\Delta f_1^K(t) \ll f_1^K(t)$ . Thus we can treat both  $\Delta_{\pi\pi}(t)$  and  $\Delta f_1^K(t)$  as small. Then, Eq. (14) can be written to leading order in the above small parameters as

$$A_{Exp,1} \approx \frac{\int_0^\infty dt [\Delta f_1^K(t) \Sigma_{\pi\pi}(t) + f_1^K(t) \Delta_{\pi\pi}(t)]}{\int_0^\infty dt \ f_1(t) \Sigma_{\pi\pi}(t)} \equiv A_{Exp,1}^{\det} + A_{Exp,1}^K \ , \tag{17}$$

where we define:

$$A_{Exp,1}^{\det} = \frac{\int_0^\infty dt \ \Delta f_1^K(t) \Sigma_{\pi\pi}(t)}{\int_0^\infty dt \ f_1^K(t) \Sigma_{\pi\pi}(t)}, \qquad A_{Exp,1}^K = \frac{\int_0^\infty dt \ f_1^K(t) \Delta_{\pi\pi}(t)}{\int_0^\infty dt \ f_1^K(t) \Sigma_{\pi\pi}(t)}.$$
(18)

The result for  $A_2$  can be obtained from Eq. (14) by  $K \leftrightarrow \overline{K}$  and P=2. This leads to

$$A_{Exp,2}^{\det} = -\frac{\int_0^{\infty} dt \ \Delta f_2^{\overline{K}}(t) \Sigma_{\pi\pi}(t)}{\int_0^{\infty} dt \ f_2^{\overline{K}}(t) \Sigma_{\pi\pi}(t)}, \qquad A_{Exp,2}^K = -\frac{\int_0^{\infty} dt \ f_2^{\overline{K}}(t) \Delta_{\pi\pi}(t)}{\int_0^{\infty} dt \ f_2^{\overline{K}}(t) \Sigma_{\pi\pi}(t)}.$$
(19)

The situation for  $A_3$  is more involved and it is discussed in Section IV.

As defined before,  $A_{Exp,P}^{\text{det}}$  is the asymmetry due to the different detection efficiency for  $\tau^+$  and  $\tau^-$  decay products. This effect is well known for decay processes into a single neutral kaon and we do not discuss it much here. However, we mention some subtitles in section VI.

The asymmetry  $A_{Exp,P}^{K}$  is the CP violation due to kaon oscillation. We turn next to study it.

## C. Kaon decay rates

The asymmetry  $A_{Exp,P}^K$  defined in Eq. (14) can be computed using the decay rates of the kaon interaction eigenstates into two pions. For applications in a realistic experiment we need to take into account the effect of kaons oscillation in matter. Such effects were studied in the past and are also known as kaons regeneration in matter [6–14].

The kaon mass eigenstates are defined as

$$|K_S\rangle = p|K^0\rangle + q|\overline{K}^0\rangle, \qquad |K_L\rangle = p|K^0\rangle - q|\overline{K}^0\rangle,$$
 (20)

with masses  $m_S$  and  $m_L$  and widths  $\Gamma_S$  and  $\Gamma_L$ . Moreover, we define the experimentally known parameters:

$$m = \frac{m_S + m_L}{2}, \qquad \Gamma = \frac{\Gamma_S + \Gamma_L}{2},$$
 (21)

$$\Delta m = m_L - m_S, \qquad \Delta \Gamma = \Gamma_L - \Gamma_S,$$
 (22)

and

$$A_S = \langle \pi \pi | H | K_S \rangle, \qquad A_L = \langle \pi \pi | H | K_L \rangle,$$
 (23)

as the decay amplitude for the mass eigenstates into two pions. We also define

$$x = \frac{\Delta m}{\Gamma}, \qquad y = \frac{\Delta \Gamma}{2\Gamma} \,.$$
 (24)

In the case where direct CP violation can be neglected, see, for example, Ref. [15], we have

$$\frac{|p|^2 - |q|^2}{|p|^2 + |q|^2} = 2\operatorname{Re}[\epsilon], \qquad \frac{\operatorname{Im}[\epsilon]}{\operatorname{Re}[\epsilon]} = -\frac{x}{y}.$$
 (25)

The equations of motion for a neutral kaon state,

$$|\psi(t)\rangle = c(t)|K^0\rangle + \overline{c}(t)|\overline{K}^0\rangle = c_S(t)|K_S\rangle + c_L(t)|K_L\rangle, \tag{26}$$

are decoupled in vacuum:

$$c_S^{\text{vac}}(t) = c_S^0 e^{-im_S t - \frac{\Gamma_S}{2}t}, \qquad c_L^{\text{vac}}(t) = c_L^0 e^{-im_L t - \frac{\Gamma_L}{2}t},$$
 (27)

where t is the time in the kaon frame, and  $c_S^0$  and  $c_L^0$  are the initial conditions of the time evolution.

When a neutral kaon state propagates in matter, it can scatter by the strong interaction with the nuclei present in the material. In general, such scattering amplitude distinguishes

between the interaction eigenstates  $K^0$  and  $\overline{K}^0$ . This modifies the Hamiltonian of the system in basis of the mass eigenstates  $K_S, K_L$  with an additional matter interaction term:

$$H_{K,\text{matter}} = \frac{1}{2} \begin{pmatrix} \chi + \overline{\chi} & \chi - \overline{\chi} \\ \chi - \overline{\chi} & \chi + \overline{\chi} \end{pmatrix}, \qquad (28)$$

where  $\chi, \overline{\chi}$  are defined in terms of the nuclear scattering amplitudes  $\mathcal{A}$  and  $\overline{\mathcal{A}}$  of the  $K^0$  and  $\overline{K}^0$  with matter [6]:

$$\chi = -\frac{2\pi n}{m_K} \mathcal{A} , \qquad \overline{\chi} = -\frac{2\pi n}{m_K} \overline{\mathcal{A}} , \qquad (29)$$

where n is the scattering centers density, and  $m_K$  is the neutral kaon mass (note that the amplitudes  $\mathcal{A}, \overline{\mathcal{A}}$  are commonly called  $f, \overline{f}$  in the literature). We also define the so called kaons regeneration parameter:

$$r = \frac{1}{2} \frac{\chi - \overline{\chi}}{\Delta m - i\Delta \Gamma/2} \,. \tag{30}$$

The value of r is typically of the order of  $10^{-2}$  or less [6, 8, 10] and can be treated as a small parameter. Solving the equations of motion for a neutral kaon state propagating in matter and neglecting  $\mathcal{O}(r^2)$  and  $\mathcal{O}(r\epsilon)$  terms we find (see for example Ref. [6])

$$c_{S}(t) = e^{-\frac{i}{2}(\chi + \overline{\chi})t} \left[ c_{S}^{0} e^{-im_{S}t - \frac{\Gamma_{S}}{2}t} + rc_{L}^{0} \left( e^{-im_{L}t - \frac{\Gamma_{L}}{2}t} - e^{-im_{S}t - \frac{\Gamma_{S}}{2}t} \right) \right] ,$$

$$c_{L}(t) = e^{-\frac{i}{2}(\chi + \overline{\chi})t} \left[ c_{L}^{0} e^{-im_{L}t - \frac{\Gamma_{L}}{2}t} + rc_{S}^{0} \left( e^{-im_{L}t - \frac{\Gamma_{L}}{2}t} - e^{-im_{S}t - \frac{\Gamma_{S}}{2}t} \right) \right] .$$
(31)

Eq. (31) can be used to compute the time evolution of the kaon interaction eigenstates  $|K^0(t)\rangle$  and  $|\overline{K}^0(t)\rangle$  created in the  $\tau$  decay processes of our interest, and to find the kaon decay rates into two pions, that include regeneration effects. We find

$$\Gamma_{\pi\pi}(t) = \frac{|A_S|^2}{4|p|^2} \left| e^{-\frac{i}{2}(\chi + \overline{\chi})t} \right|^2 \left[ -2\operatorname{Re}[r] \left( e^{-\Gamma_s t} - e^{-\Gamma t} \left( \cos(\Delta m t) + \frac{\operatorname{Im}[r]}{\operatorname{Re}[r]} \sin(\Delta m t) \right) \right) + e^{-\Gamma_s t} - 2\operatorname{Re}[\epsilon] e^{-\Gamma t} \left( \cos(\Delta m t) + \frac{\operatorname{Im}[\epsilon]}{\operatorname{Re}[\epsilon]} \sin(\Delta m t) \right) \right], \quad (32)$$

and

$$\overline{\Gamma}_{\pi\pi}(t) = \frac{|A_S|^2}{4|q|^2} \left| e^{-\frac{i}{2}(\chi + \overline{\chi})t} \right|^2 \left[ -2\operatorname{Re}[r] \left( -e^{-\Gamma_s t} + e^{-\Gamma t} \left( \cos(\Delta m t) + \frac{\operatorname{Im}[r]}{\operatorname{Re}[r]} \sin(\Delta m t) \right) \right) + e^{-\Gamma_s t} + 2\operatorname{Re}[\epsilon] e^{-\Gamma t} \left( \cos(\Delta m t) + \frac{\operatorname{Im}[\epsilon]}{\operatorname{Re}[\epsilon]} \sin(\Delta m t) \right) \right].$$
(33)

where we have used  $A_L/A_S \approx \epsilon$ . As a consequence, we find that to leading order

$$\Sigma_{\pi\pi}(t) = Ce^{-\Gamma_S t} \,, \tag{34}$$

and that

$$\Delta_{\pi\pi}(t) = C \left[ \left( -2\operatorname{Re}[\epsilon] - 2\operatorname{Re}[r] \right) e^{-\Gamma_S t} + 2\operatorname{Re}[r] e^{-\Gamma t} \left( \cos(\Delta m t) + \frac{\operatorname{Im}[r]}{\operatorname{Re}[r]} \sin(\Delta m t) \right) + 2\operatorname{Re}[\epsilon] e^{-\Gamma t} \left( \cos(\Delta m t) - \frac{x}{y} \sin(\Delta m t) \right) \right], \quad (35)$$

where we defined

$$C = \frac{|A_S|^2}{4} \frac{|p|^2 + |q|^2}{|p|^2 |q|^2} \left| e^{-\frac{i}{2}(\chi + \overline{\chi})t} \right|^2.$$
 (36)

Using Eq. (29) and the optical theorem,  $\chi, \overline{\chi}$  can be related to the total interaction cross sections of  $K^0$  and  $\overline{K}^0$  with matter, see for example Ref. [6]. For applications in realistic experiments, such cross sections are small, and the factor  $\left|e^{-\frac{i}{2}(\chi+\overline{\chi})t}\right|^2\approx 1$  can be ignored up to small corrections. At leading order in  $\epsilon$  and r we can separate the asymmetry due to kaons oscillation into two contributions:

$$A_{Exp,P}^{K} = A_{Exp,P}^{K,\text{vac}} + A_{Exp,P}^{K,\text{mat}}$$
 (37)

The asymmetry  $A_{Exp,P}^{K,\text{vac}}$  is due to kaons oscillation in vacuum, that is when r=0, and only depends on the CP violating parameter  $\epsilon$ ,

$$A_{Exp,1}^{K,\text{vac}} = -2\text{Re}[\epsilon] \left[ 1 - \frac{\int_0^\infty dt \ f_1^K(t)e^{-\Gamma t} \left(\cos(\Delta mt) - \frac{x}{y}\sin(\Delta mt)\right)}{\int_0^\infty dt \ f_1^K(t)e^{-\Gamma st}} \right] . \tag{38}$$

The term  $A_{Exp,P}^{K,\text{mat}}$ , is the correction to the kaons oscillation asymmetry due to kaons regeneration in matter, and only depends on the parameter r, which depends on the properties of the material used in the experiment. We discuss this correction in Section VI.

For an ideal experiment, where  $f_1^K(t) = 1$ , and the oscillation happens in vacuum, r = 0, the integrals in Eq. (38) can be performed analytically and we obtain

$$A_{Ideal,1}^{K} = -2\operatorname{Re}[\epsilon] \frac{\Gamma_{S} \left( x\Delta m\Gamma_{S} + y\Delta m^{2} + y\Gamma^{2} - y\Gamma\Gamma_{S} \right)}{y(\Delta m^{2} + \Gamma^{2})} . \tag{39}$$

Using the definitions in Eq. (24), and that from  $\Gamma_S \gg \Gamma_L$  we have  $\Delta\Gamma \approx -\Gamma_S$ , we can rewrite Eq. (39) in terms of x and y only:

$$A_{Ideal,1}^{K} = -2\operatorname{Re}[\epsilon] \frac{2y^2 + yx^2 - y}{yx^2 + y} \approx +2\operatorname{Re}[\epsilon] , \qquad (40)$$

where in the last step we have used  $x \approx -y$  and  $x \approx 1$ , as known from experimental kaons oscillation data. We note that while numerically the result agrees with that of [1] this is just a numerical accident.

The generalization to the case of  $A_2$  is straightforward and we get

$$A_{Exp,2}^{\text{det}} = \frac{\int_0^\infty dt \ \Delta f_2^{\overline{K}}(t) e^{-\Gamma_S t}}{\int_0^\infty dt \ f_2^{\overline{K}}(t) e^{-\Gamma_S t}},\tag{41}$$

and

$$A_{Exp,2}^{K,\text{vac}} = +2\text{Re}[\epsilon] \left[ 1 - \frac{\int_0^\infty dt \ f_2^{\overline{K}}(t)e^{-\Gamma t} \left(\cos(\Delta mt) - \frac{x}{y}\sin(\Delta mt)\right)}{\int_0^\infty dt \ f_2^{\overline{K}}(t)e^{-\Gamma st}} \right] , \tag{42}$$

which shows that in an ideal experiment in vacuum with perfect deficiency  $f_1^K(t) = f_2^{\overline{K}}(t) = 1$ , we would have  $A_2 = -A_1$ .

#### III. THE EFFICIENCY FUNCTION

The efficiency is a function of the kaon decay time t in the kaon rest frame. As seen in Eq. (6) it depends on three indices. In this section, to simplify the notation, we write the efficiency function as  $f_P^{\alpha}(t)$ , where we define the multi-index  $\alpha$  to be

$$\alpha = (+, K), \ (+, \overline{K}), \ (-, K), \ (-, \overline{K}),$$
 (43)

such that it defines whether we consider the efficiency for  $K^0$  or  $\overline{K}^0$ , and whether the kaon is coming from  $\tau^+$  or  $\tau^-$  decay.

## A. Obtaining the efficiency function

The efficiency function fundamentally depends on the kaon spectrum in the  $\tau$  rest frame as well as the detector details and performance.

To understand how we obtain  $f_P^{\alpha}(t)$ , we first note that we have to consider three different frames: the kaon frame, the  $\tau$  frame, and the laboratory (lab) frame. The fundamental two functions that define the efficiency function are:

•  $F(L, E, \vec{p}, X_{\alpha})$ : the laboratory efficiency function. It gives the reconstruction efficiency of the experiment for the detection of a neutral kaon, as a function of the kaon decay

length L, energy E, momentum  $\vec{p}$ , and any other relevant parameters collected in the multivariable symbol  $X_{\alpha}$ , in the laboratory frame.

•  $S_{\alpha,P}^{(\tau)}(E^{(\tau)}, \hat{n}^{(\tau)})$ : the normalized kaon energy spectrum in the  $\tau$  rest frame. It is a function of the energy,  $E^{(\tau)}$ , and direction,  $\hat{n}^{(\tau)} = \vec{p}^{(\tau)}/p^{(\tau)}$ , of the kaon emitted in the process P in the  $\tau$  frame.

# We further define

•  $S_{\alpha,P}(E,\hat{n})$ : The normalized kaon energy spectrum in the laboratory frame. It is a function of the energy, E, and direction,  $\hat{n} = \vec{p}/p$ , of the kaon emitted in the process P in the laboratory frame.

We obtain the laboratory frame spectrum,  $S_{\alpha,P}$  from the spectrum in the  $\tau$  frame,  $S_{\alpha,P}^{(\tau)}$ , by considering a boost from the  $\tau$  frame to the laboratory frame:

$$(E, \vec{p}) = \operatorname{Boost}_{\tau \to LAB}(E^{(\tau)}, \vec{p}^{(\tau)}). \tag{44}$$

The boost depends on the direction and velocity of the  $\tau$  in the laboratory frame.

In general, the computation of the laboratory-frame spectrum  $S_{\alpha,P}$  is nontrivial, since the velocity and angular distribution of the  $\tau$  depend on both the center-of-mass energy and the asymmetry of the machine. While this is usually not an issue, the presence of neutrinos in the final state makes it problematic. Otherwise, one could simply combine all the daughter particles to reconstruct the  $\tau$  momentum and direction. In practice, the spectrum must therefore be determined using numerical methods.

We express the efficiency as a function of the decay proper time in the kaon rest frame, t. The corresponding decay length in the laboratory frame can be written as  $L = \beta \gamma t$ , where  $\beta$  denotes the kaon velocity in the laboratory frame and  $\gamma = 1/\sqrt{1-\beta^2}$  is the relativistic time dilatation factor. Both  $\beta$  and  $\gamma$  depend on the energy in the laboratory frame. Similarly, we can parametrize the additional parameters as  $X_{\alpha} = X_{\alpha}(t)$ . The total detection efficiency is then obtained by averaging over the energy and momentum distribution of the kaon produced in process P in the laboratory frame:

$$f_P^{\alpha}(t) = \int d\Omega \, dE \, S_{\alpha,P}(E,\hat{n}) \, F(\beta \gamma t, E, \vec{p}, X_{\alpha}(t)) \,, \tag{45}$$

where  $\Omega$  is the solid angle.

Eq. (45) is the main result of this section. It shows that the efficiency function  $f_P^{\alpha}(t)$  factorizes into two components: the kaon spectrum  $S_{\alpha,P}(E,\hat{n})$  in the laboratory frame, which depends on the specific process P; and a universal laboratory frame reconstruction efficiency  $F(L, E, \vec{p}, X_{\alpha})$ , which depends only on the experiment conditions. To move forward we need to understand the detector as well as the spectrum. Yet, many of the results can follow assuming a simplified version of both, as we turn to next.

# B. Simplification functions

In this subsection we make simplification approximations. We assume that F is only a function of the kaon decay length and energy in the laboratory frame, F = F(L, E). Since in this case F does not depend on  $\alpha$ , it does not have any additional CP violating effects. We can then use the kaon rest frame decay time, and the laboratory frame energy of the kaon to write it as  $F(\beta \gamma t, E)$ . Under this assumption, the efficiency function is parameterized by the kaon decay time t in its rest frame:

$$f_P^{\alpha}(t) = \int dE \ S_{\alpha,P}(E) F(\beta \gamma t, E). \tag{46}$$

Eq. (46) shows that in this simplified case, the reconstruction efficiency  $f_P^{\alpha}$  depends on the energy distribution of the kaon, which depends on the specific process and kaon in final state  $(\alpha, P)$ , and on F(L, E), that is a universal experimental function, that does not depend on the process and on the kaon detected in final state.

To illustrate the effect, we introduce a simple model that captures the essential features of the experiment. Specifically, we impose fixed decay-length cuts,  $L_1$  and  $L_2$ , in the laboratory frame to describe the finite geometrical acceptance of a particular detector,

$$F(L,E) = F^{(L_1,L_2)}(L) = \theta (L - L_1) \theta (-L + L_2) , \qquad (47)$$

where  $\theta$  is the step function. This represents a simplified case in which the laboratory frame efficiency function F(L, E) depends solely on the decay length L. For the above function, the time cuts in the kaon frame are energy-dependent. Given the efficiency  $F(L, E) = F^{(L_1, L_2)}(L)$  as a simple geometrical acceptance model, we consider the case P = 1 of the asymmetry  $A_1$ , where there is a single neutral kaon in the final state. Moreover, we assume that there is no direct CP violation the  $\tau$  decay, that the kaon oscillations happens in

vacuum,  $A_{Exp,1}^K = A_{Exp,1}^{1,\text{vac}}$ , and we neglect a small effect by assuming that  $\Delta f_1^K(t) = 0$ , which means that the spectrum  $S_{1,K}^+(E)$  of the  $K^0$  emitted by  $\tau^+$ , is the same as the spectrum  $S_{1,\overline{K}}^-(E)$  of the  $\overline{K}^0$  emitted by  $\tau^-$ . As a consequence, we can drop the index  $\alpha$ , and only consider  $f_1^K(t) = f_1(t)$ , see Eq. (11). Under these assumptions, the experimentally accessible asymmetry  $A_{Exp,1} = A_{Exp,1}^{K,\text{vac}} = A_{Exp,1}^{(L_1,L_2)}$  is given by Eq. (14), where the kaon rest frame efficiency function takes the form

$$f_1^{(L_1, L_2)}(t) = \int S_1(E) \,\theta\left(t - \frac{L_1}{\beta\gamma}\right) \theta\left(-t + \frac{L_2}{\beta\gamma}\right) dE. \tag{48}$$

To study the impact of the efficiency function on the experimental asymmetry, and its dependence on the kaons energy, we consider a simplified toy model in which the kaons are emitted with a fixed laboratory-frame energy  $E_0$ . In this case the spectrum reduces to

$$S_1 = \delta(E - E_0). \tag{49}$$

The efficiency function gives fixed-time experimental cuts that depends on the energy,

$$f_1^{(L_1, L_2)}(t) = \theta \left( t - \frac{L_1}{\beta \gamma} \right) \theta \left( -t + \frac{L_2}{\beta \gamma} \right), \tag{50}$$

where  $\beta \gamma = \sqrt{E_0^2 - m_K^2}/m_K$ . Using Eq. (14), the asymmetry  $A_{Exp,1}^{(L_1,L_2)}(E_0)$  modifies as

$$A_{Exp,1}^{(L_1,L_2)}(E_0) = \frac{\int_{L_1/\beta\gamma}^{L_2/\beta\gamma} dt \left[\Gamma_{\pi\pi}(t) - \overline{\Gamma}_{\pi\pi}(t)\right]}{\int_{L_1/\beta\gamma}^{L_2/\beta\gamma} dt \left[\Gamma_{\pi\pi}(t) + \overline{\Gamma}_{\pi\pi}(t)\right]}.$$
 (51)

As illustrated by eq. (51), the kaons emitted with different energies, have different efficiency functions, and, as a consequence, a different measured asymmetry  $A_{Exp,1}^{(L_1,L_2)}(E_0)$ . Using Eq. (38), the asymmetry can be written as

$$A_{Exp,1}^{(L_1,L_2)}(E_0) = -2\text{Re}[\epsilon] \left(1 - \frac{I_{\text{int}}}{I_{\text{tot}}}\right) ,$$
 (52)

with

$$I_{\text{int}} = \int_{L_1/\beta\gamma}^{L_2/\beta\gamma} dt \, \exp(-\Gamma t) \left[ \cos(\Delta m t) - \frac{x}{y} \sin(\Delta m t) \right], \tag{53}$$

$$I_{\text{tot}} = \int_{L_1/\beta\gamma}^{L_2/\beta\gamma} dt \, \exp\left(-\Gamma_S t\right). \tag{54}$$

Fig. 1 displays the asymmetry  $A_{Exp,1}^{(L_1,L_2)}(E_0)$  for different fixed values of the kaon energy  $E_0$  in the laboratory frame, as a function of the decay length  $L_2$  of the experiment. In contrast, Fig. 2 shows the asymmetry  $A_{Exp,1}^{(L_1,L_2)}(E_0)$  as a function of  $E_0$  for fixed values of  $L_1$  and  $L_2$ .

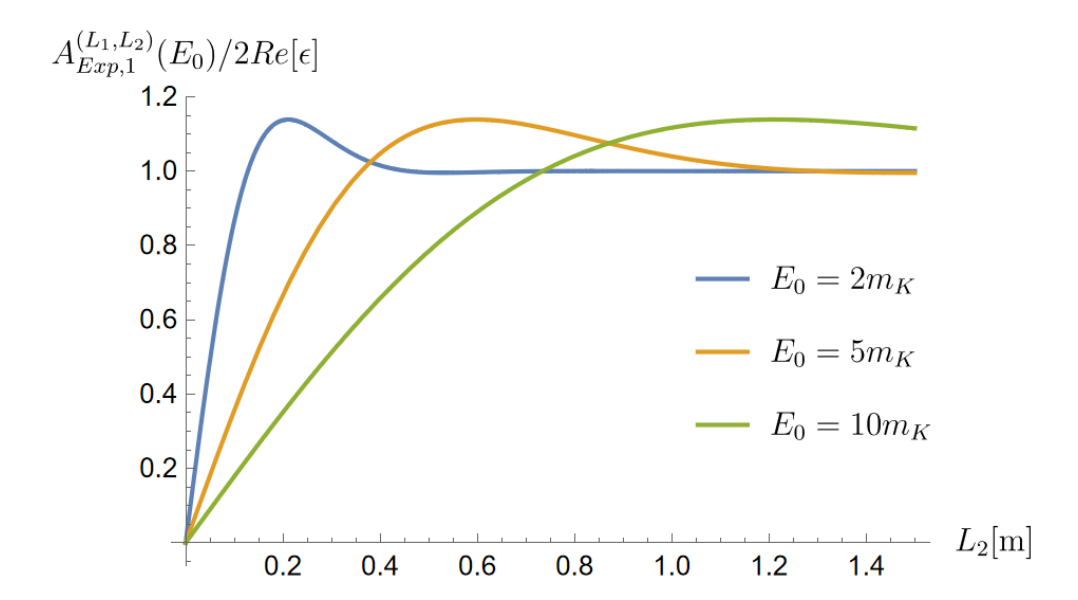


FIG. 1: The asymmetry  $A_{Exp,1}^{(L_1,L_2)}(E_0)$  as a function of the total length of the experiment  $L_2$  for different values of the kaon energy  $E_0$ . In this plot we set  $L_1 = \tau_S c/10 \approx 3$ mm, noting that for Belle II the average energy of the emitted kaons is  $\langle E \rangle \approx 5 m_{K^0}$ , with tails of the spectrum extending up to approximately  $10 m_{K^0}$ .

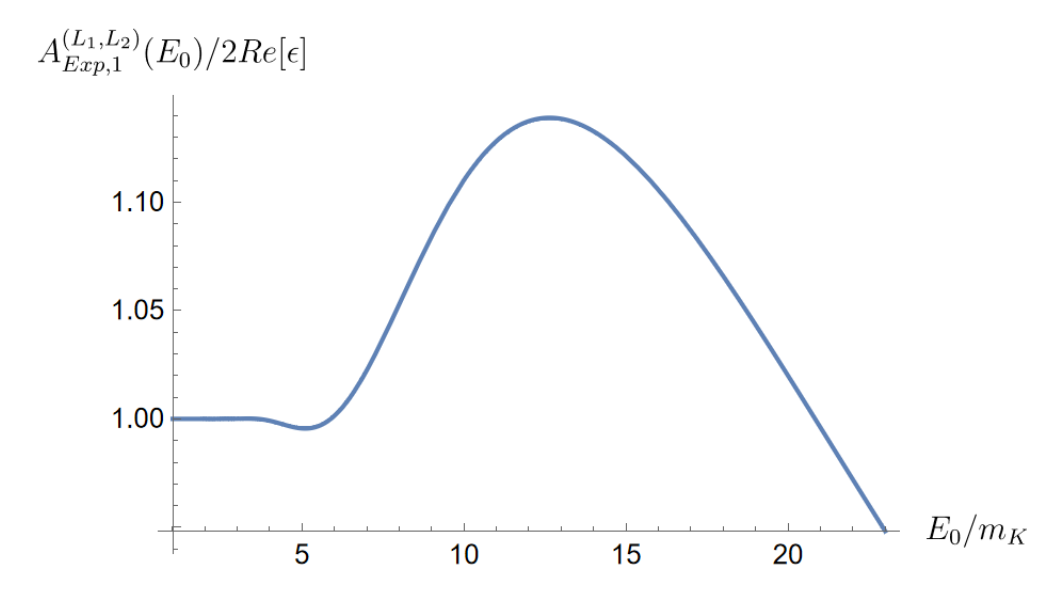


FIG. 2: The asymmetry  $A_{Exp,1}^{(L_1,L_2)}(E_0)$  as a function of the kaon energy  $E_0$ . In this plot we set  $L_1 = \tau_S c/10 \approx 3 \text{mm}$  and  $L_2 = \tau_L c/10 \approx 1.5 \text{m}$ .

#### IV. CP VIOLATION IN DECAYS INVOLVING TWO NEUTRAL KAONS

We now consider the case of the  $A_3$  asymmetry, Eq. (4). In terms of the kaon interaction eigenstates created, we are looking at the process  $\tau \to \pi K^0 \overline{K}^0 \nu$ , where the  $K^0$  and  $\overline{K}^0$  pairs are identified as  $K_S$  and  $K_L$  pairs. As before, we consider the case where the  $K_S$  is identified by a  $\pi\pi$  system in the final state, while the  $K_L$  is identified as missing in the final detection due to its long lifetime. This process is particularly relevant because it contributes as a background to the  $A_1$  measurement. The difference in this case compared to  $A_1$  and  $A_2$  discussed earlier is that, because there are two neutral kaons,  $K^0$  and  $\overline{K}^0$ , in the final state, we have to consider four possible different efficiency functions, denoted as  $f_P^{+,K}(t)$ ,  $f_P^{-,K}(t)$ ,  $f_P^{-,K}(t)$ ,  $f_P^{-,K}(t)$ . In general, the difference between the  $K^0$  and  $\overline{K}^0$  efficiency functions makes the CP asymmetry ratio, Eq. (4), non-vanishing.

For an ideal experiment without cuts and perfect efficiency,  $A_3$  is zero. The reason is that, since both  $K^0$  and  $\overline{K}^0$  are produced, the probability to have a  $\pi\pi$  system in the final state is the same for  $\tau^+$  and  $\tau^-$  decay. In realistic experiments, however, finite efficiency introduces artificial asymmetry. In particular, this arises because the efficiency functions  $f_P^K(t)$  and  $f_P^{\overline{K}}(t)$  depend on the kaons spectrum. The kaon interaction eigenstates  $K^0$  and  $\overline{K}^0$  are produced with a different energy spectra in  $\tau$  decay. Thus, a more energetic  $K^0$  has a different probability of arising from a  $\tau^+$  compared to a  $\tau^-$ . As a consequence, the experimental cuts can bias the number of  $K_S$  originating from  $\tau^+$  and  $\tau^-$ .

To make this explicit, we consider the case where  $K^0$  and  $\overline{K}^0$  are emitted with a different energy spectra in the  $\tau^{\pm} \to \nu K^0 \overline{K}^0 \pi^{\pm}$  process. We define  $S_K^{\pm}(E)$  and  $S_{\overline{K}}^{\pm}(E)$  as the energy spectra of the  $K^0$  and the  $\overline{K}^0$  emitted in the decay of the  $\tau^{\pm}$  in the laboratory frame. Note that, to simplify the notation, the subscript P=3 is implicit. The experimentally measured asymmetry  $A_3$  is then given by

$$A_{Exp,3} = \frac{\int_0^\infty dt \, \left[ \left( f_3^{+,K}(t) \Gamma_{\pi\pi}(t) + f_3^{+,\overline{K}}(t) \overline{\Gamma}_{\pi\pi}(t) \right) - \left( f_3^{-,K}(t) \Gamma_{\pi\pi}(t) + f_3^{-,\overline{K}}(t) \overline{\Gamma}_{\pi\pi}(t) \right) \right]}{\int_0^\infty dt \, \left[ \left( f_3^{+,K}(t) \Gamma_{\pi\pi}(t) + f_3^{+,\overline{K}}(t) \overline{\Gamma}_{\pi\pi}(t) \right) + \left( f_3^{-,K}(t) \Gamma_{\pi\pi}(t) + f_3^{-,\overline{K}}(t) \overline{\Gamma}_{\pi\pi}(t) \right) \right]} . \tag{55}$$

Assuming that direct CP violation in  $\tau$  decays is negligible, we can write

$$S_K^+(E) = S_{\overline{K}}^-(E), \qquad S_K^-(E) = S_{\overline{K}}^+(E).$$
 (56)

Thus, in the following we omit the + superindex and make it implicit:

$$S_K = S_K^+, \qquad S_{\overline{K}} = S_{\overline{K}}^+. \tag{57}$$

Note that while Eq. (56) is exact in the  $\tau$  rest frame, small deviations may arise in the laboratory frame due to effects such as the forward-backward asymmetry in the  $\tau^+\tau^-$  production (see Section VI). These corrections, however, are subleading and can be neglected in the present analysis.

From the efficiency function Eq. (45), we then obtain

$$f_3^{+,K}(t) = f_3^{-,\overline{K}}(t) = f_3^K(t) , \qquad f_3^{+,\overline{K}}(t) = f_3^{-,K}(t) = f_3^{\overline{K}}(t) .$$
 (58)

As a consequence, only the two efficiency functions  $f_3^K(t)$  and  $f_3^{\overline{K}}(t)$  defined in Eq. (9) are relevant.

To demonstrate the effect, we consider the simplified case where the reconstruction efficiency of the detector in the laboratory frame is given by F(L, E). Then, using Eq. (46), the kaon frame efficiency function for the  $K^0$  and  $\overline{K}^0$  emitted by the  $\tau^+$  are

$$f_3^K(t) = \int dE \, S_K(E) F(\beta \gamma t, E), \qquad f_3^{\overline{K}}(t) = \int dE \, S_{\overline{K}}(E) F(\beta \gamma t, E) .$$
 (59)

Using Eq. (58), the asymmetry can be rewritten as

$$A_{Exp,3} = \frac{\int_0^\infty dt \, \left[ \left( f_3^K(t) \Gamma_{\pi\pi}(t) + f_3^{\overline{K}}(t) \overline{\Gamma}_{\pi\pi}(t) \right) - \left( f_3^{\overline{K}}(t) \Gamma_{\pi\pi}(t) + f_3^K(t) \overline{\Gamma}_{\pi\pi}(t) \right) \right]}{\int_0^\infty dt \, \left[ \left( f_3^K(t) \Gamma_{\pi\pi}(t) + f_3^{\overline{K}}(t) \overline{\Gamma}_{\pi\pi}(t) \right) + \left( f_3^{\overline{K}}(t) \Gamma_{\pi\pi}(t) + f_3^{\overline{K}}(t) \overline{\Gamma}_{\pi\pi}(t) \right) \right]}, \quad (60)$$

and using Eq. (16),

$$A_{Exp,3} = \frac{\int_0^\infty dt \ f_3^K(t) \Delta_{\pi\pi}(t) - \int_0^\infty dt \ f_3^{\overline{K}}(t) \Delta_{\pi\pi}(t)}{\int_0^\infty dt \ f_3^K(t) \Sigma_{\pi\pi}(t) + \int_0^\infty dt \ f_3^{\overline{K}}(t) \Sigma_{\pi\pi}(t)} \ . \tag{61}$$

This expression can be rewritten in a more convenient form as

$$A_{Exp,3} = \frac{\int_0^\infty dt \ \Delta f_3(t) \Delta_{\pi\pi}(t)}{\int_0^\infty dt \ f_3(t) \Sigma_{\pi\pi}(t)},\tag{62}$$

where the efficiency functions  $f_P(t)$  and  $\Delta f_P(t)$  with no superindex are defined in Eq. (11). The term  $\Delta f_3(t)$  quantifies the difference between the efficiency functions for  $K^0$  and  $\overline{K}^0$ , reflecting their different energy spectra in the  $\tau^+$  decay, see Eq. (59). This contrasts with  $A_{Exp,1}^{\text{det}}$  defined in Eq. (18), where the efficiency differences between two CP conjugates modes arise from detector-related effects.

We emphasize that  $A_3 \neq 0$  originates from the different energy spectra of  $K^0$  and  $\overline{K}^0$  in the  $\tau$  rest frame, which translates into different spectra also in the laboratory frame:  $S_K(E) \neq S_{\overline{K}}(E)$ . Consequently, the dependence of  $f_P(t)$  on the energy spectrum, see Eq. (46), prevents cancellation of asymmetries. Indeed, if  $S_K = S_{\overline{K}}$ , then  $\Delta f(t) = 0$ , and  $A_3$  would vanish. In contrast,  $A_1$  and  $A_2$  correspond to genuine physical asymmetries that would exist even with perfect detection efficiency  $F(L, E) = f_P(t) \equiv 1$ . By comparison,  $A_3$  arises solely from the limited reconstruction efficiency of the experiment.

## V. RELEVANCE FOR BELLE II

In this section we discuss the SM predictions for the asymmetries  $A_1$ ,  $A_2$ , and  $A_3$  relevant to a Belle II-type experiment [5]. We emphasize that this constitutes a simplifying analysis and a complete analysis must be carried out in conjunction with the experimental data. As shown in Eq. (45), the calculation requires knowledge of the detector efficiency function F as well as the spectra of  $K^0$  and  $\overline{K}^0$  mesons produced in  $\tau$  decays across the different processes.

### A. Belle II Efficiency Function

To compute the reconstruction efficiency function for a Belle II-type experiment, we adopt the simplified model of Eq. (46), in which the laboratory-frame efficiency function F is assumed to depend only on the decay length L and the energy E of the detected kaon, F = F(L, E).

We generate  $10^7 K_S$  mesons under Belle II kinematics constraints. For each  $K_S$ , we simulate the decay length L, the decay time t in the kaon rest frame, and the laboratory-frame energy E. The full sample is then divided into equipopulous 10 bins of laboratory-frame energy  $\Delta E_i$ . For each bin  $\Delta E_i$ , we construct the decay-time distribution. These distributions are subsequently smeared to mimic the resolution effects, providing a set of reference distributions, denoted  $D_i^0(t)$ . In this approximate model, the detector efficiency F is parameterized as

$$F(L, E) = F_i(L) \text{ for } E \in \Delta E_i = [E_i, E_{i+1}] \quad i = 1, ..., 10.$$
 (63)

To each decay-time distribution  $D_i^0(t)$ , we apply experimental cuts given by the acceptance

of the detector and by selection analysis typical of a Belle II like experiment:

$$\begin{cases}
0.3 < \theta(\pi^{\pm})[\text{rad}] < 2.62 , \\
0.2 < p_T(K_S)[\text{GeV}] < 4.5 , \\
p_T(\pi^{\pm})[\text{GeV}] > 0.1 , \\
K_S \text{ decay length[cm]} > 0.2
\end{cases}$$
(64)

where  $\theta$  is the angle with respect to the beam pipe, and  $p_T = p \sin \theta$  is the transverse momentum. Moreover, in order to reproduce the loss of efficiency for higher decay times of the  $K_S$ , we model the vertex fitting efficiency as a linear function of the flight distance in the range [0.2, 120] cm. This yields a new set of distributions  $D_i^{exp}(t)$ , which mimic those expected in experimental data.

The efficiency in each bin is then extracted as a function of decay length, expressed in terms of the boosted decay time  $L = \beta \gamma t$ , by measuring the ratio:

$$F_i(\beta \gamma t) = \frac{D_i^{exp}(t)}{D_i^0(t)}, \text{ for } E \in \Delta E_i.$$
 (65)

To obtain an analytic expression of  $F_i(\beta \gamma t)$ , we fit the above ratio with the following seven-parameter function:

$$F_i(\beta \gamma t) = \begin{cases} (c_1 + c_2 e^{-c_3 t})^{c_4} & \text{for } t \in [0, t_1], \\ c_5 t^2 + c_6 t + c_7 & \text{for } t \in [t_1, t_2], \end{cases}$$
(66)

where  $c_1, ..., c_7$  are the fit parameters, each implicitly dependent on i = 1, ..., 10. The transition point  $t_1$  is determined separately for every energy range  $\Delta E_i$  to give the best fit, while the upper bound is fixed at  $t_2 = 6 \tau_S$  for all generated events. Finally, the results across all bins are combined to construct a global model for the efficiency function  $F(\beta \gamma t)$ . Fig. 3 illustrates an example of the detector efficiency obtained for the first energy bin  $\Delta E_1$ , together with the corresponding fit. The behavior in other energy bins is similar.

# B. Predictions for $A_1$ and $A_2$

As shown in Eq. (18) and Eq. (19), the experimental asymmetries  $A_{Exp,1}$  and  $A_{Exp,2}$  depend on the efficiency function  $f_P^{\alpha}(t)$ , which in turn depends on the kaon energy distribution of the

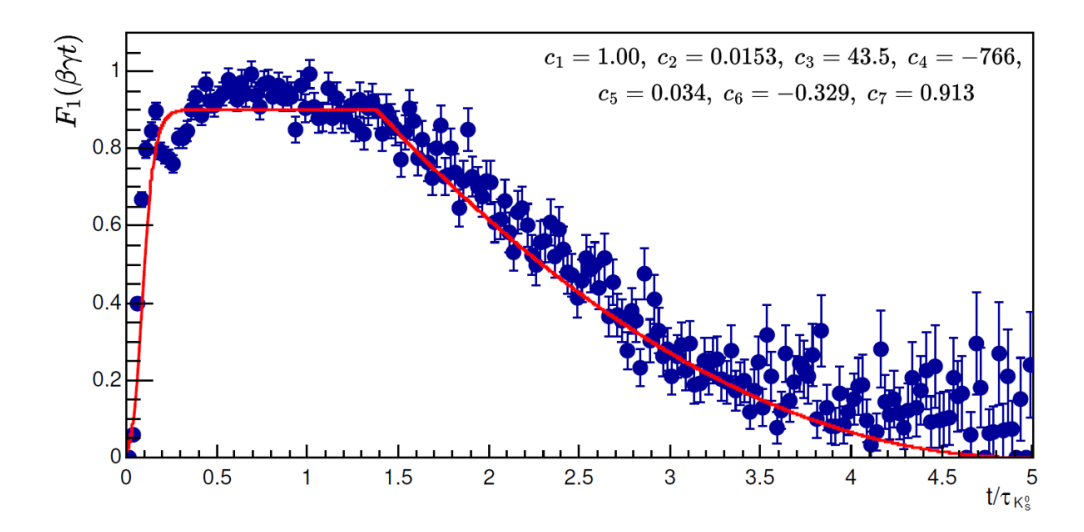


FIG. 3: Example of the approximate detector efficiency model for a Belle II-type experiment for the first energy bin  $\Delta E_1 = [0.55, 1.23]$  GeV. The red curve is the result of the fit using Eq. (66), with the fit parameters showed in the upper right of the figure.

specific decay. Since the energy spectrum of the neutral kaon in  $\tau^{\pm} \to \nu K^{\pm} K_S$  differs from that in  $\tau^{\pm} \to \nu \pi^{\pm} K_S$ , one generally expects  $A_1 \neq -A_2$  in real experimental measurements.

In the *U*-spin limit, however, the two spectra relevant for  $A_1$  and  $A_2$  become identical, leading to  $A_1 = -A_2$ . Deviations from this relation arise from *U*-spin breaking effects, which are expected to be small.

To determine the asymmetries, we first compute the efficiency functions  $f_1^K(t)$  and  $f_2^{\overline{K}}(t)$ . For simplicity, we assume that  $\Delta f_1^K = 0$  and  $\Delta f_2^{\overline{K}} = 0$ , thereby neglecting detector-related systematic effects. Furthermore, we identify the experimental asymmetries with their vacuum counterparts,  $A_{Exp,1} = A_{Exp,1}^{K,\text{vac}}$  and that  $A_{Exp,2} = A_{Exp,2}^{K,\text{vac}}$ , which amounts to neglecting matter-interactions effects. The detector efficiency is modeled according to Eq. (63), and the total efficiency functions are obtained through Eq. (46). For the case of  $A_1$ , we require the laboratory frame  $K^0$  energy spectrum  $S_{K,1}(E)$  associated with the decay  $\tau^+ \to \overline{\nu}\pi^+ K^0$  process:

$$f_1^K(t) = \sum_{i=1}^{10} \int_{\Delta E_i} dE \ S_{K,1}(E) F_i(\beta \gamma t) \ . \tag{67}$$

Similarly, for  $A_2$ , the relevant input is the laboratory frame  $\overline{K}^0$  spectrum  $S_{\overline{K},2}(E)$  from the decay the  $\tau^+ \to \overline{\nu} K^+ \overline{K}^0$  process:

$$f_2^{\overline{K}}(t) = \sum_{i=1}^{10} \int_{\Delta E_i} dE \, S_{\overline{K},2}(E) F_i(\beta \gamma t) . \qquad (68)$$

We first compute the energy spectra  $S_{K,1}^{(\tau)}$  and  $S_{\overline{K},2}^{(\tau)}$  in the  $\tau$  rest frame. For this purpose, we adopt a simplified model of a point-like three-body decay. In this approximation, the difference between the two spectra arises from the available kinematic phase space. This treatment provides only a rough estimate, sufficient to gauge the impact of kaon energy distributions on the experimental asymmetries. Further details of the spectrum computation in the  $\tau$  rest frame are given in Appendix A.

To obtain the laboratory-frame spectra,  $S_{K,1}(E)$  and  $S_{\overline{K},2}(E)$ , we boost the results from the  $\tau$  rest frame. For Belle II-type experiment, we assume an asymmetric electron-positron collider operating at an invariant mass  $\sqrt{s} = 10.58$  GeV, with the entire center-of-mass energy used for  $\tau^+\tau^-$  production. The collider asymmetry originates from the unequal beam energies, taken here as 4 GeV and 7 GeV. The angular distribution of the  $\tau^+\tau^-$  pairs in the center-of-mass frame is determined from the  $e^+e^- \to \tau^+\tau^-$  cross section.

Using the analytic expressions in Eq. (38) and Eq. (42), we obtain numerical estimates for the asymmetries:

$$A_{Exp,1} \approx 3.00 \times 10^{-3} \approx 0.909 \times 2 \text{Re}[\epsilon],$$
 (69)

$$A_{Exp,2} \approx -3.07 \times 10^{-3} \approx -0.931 \times 2 \text{Re}[\epsilon] \,.$$
 (70)

Thus, for a Belle II-type experiment the relation  $A_2 = -A_1$  holds to within an error of order:

$$\frac{A_{Exp,1} + A_{Exp,2}}{2\text{Re}[\epsilon]} \approx 2\% \ . \tag{71}$$

While we do not assign an error on the above estimate, we do expect that the result is a correct rough estimate and thus that the effect is within the range of a few percent. Thus, we conclude that this deviation is expected to remain below the experimental sensitivity.

#### C. Prediction for $A_3$

We now turn to a theoretical estimate of the experimental asymmetry  $A_{Exp,3}$ , defined in Eq. (62). This requires the evaluation of the efficiency functions  $f_3^K(t)$  and  $f_3^{\overline{K}}(t)$  from Eq. (59), and consequently  $\Delta f_3(t)$ . Hence, we need a theoretical model for the kaon energy distribution functions  $S_K(E)$  and  $S_{\overline{K}}(E)$  in the  $\tau^+$  decay, as introduced in Eq. (57).

The decay of  $\tau$  into three pseudoscalar mesons has been studied in literature [16–18]. For the present analysis, however, we aim only at a rough estimate of the possible size of the

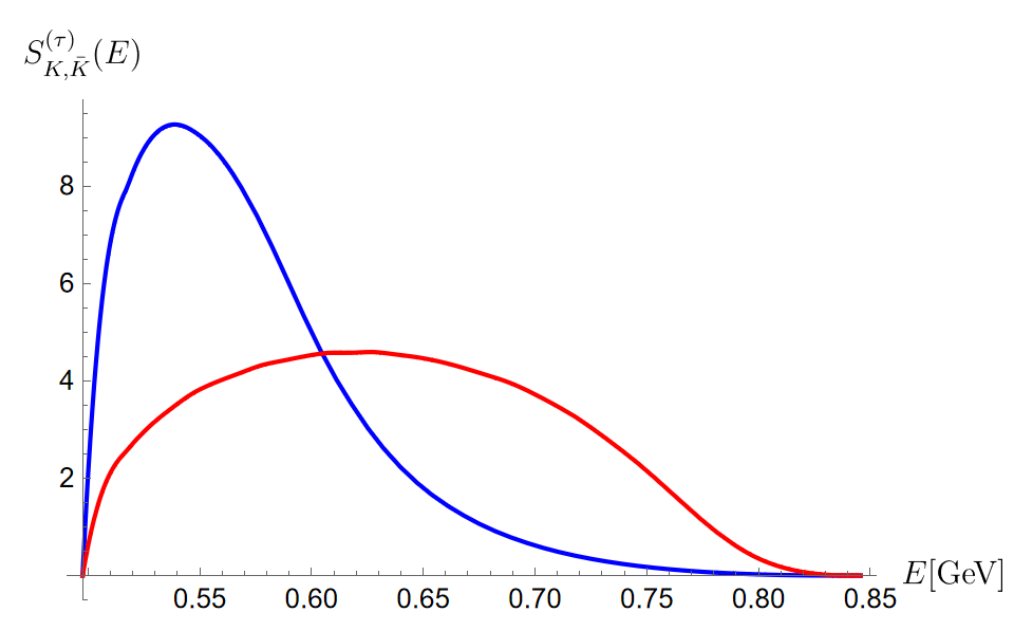


FIG. 4: Normalized energy spectra of the kaons in the decay  $\tau^+ \to \overline{\nu} \pi^+ K^0 \overline{K}^0$  in the  $\tau$  rest frame:  $S_K^{(\tau)}(E)$  for  $K^0$  (red line) and  $S_{\overline{K}}^{(\tau)}(E)$  for  $\overline{K}^0$  (blue line). A simplified interaction model with an intermediate  $K^*$  resonance is employed [16, 17].

effect. We therefore adopt a simplified model for the process  $\tau \to \nu K^0 \overline{K}^0 \pi$ . Specifically, we treat the decay as proceeding through an intermediate  $K^*$  resonance, corresponding to a pseudo-three-body decay:

$$\tau^+ \to \nu K^{*+} \overline{K}^0 \to \nu K^0 \overline{K}^0 \pi^+, \qquad \tau^+ \to \nu K^0 \overline{K}^{*+} \to \nu K^0 \overline{K}^0 \pi^+.$$
 (72)

The  $K^*$  resonance parameters are taken as [16, 17]:

$$m_{K^*} = 0.892 \text{ GeV}, \qquad \Gamma_{K^*} = 0.050 \text{ GeV}.$$
 (73)

Further details of the computation of the  $K^0$  and  $\overline{K}^0$  spectra in the  $\tau$  rest frame are provided in Appendix A. We stress that this model is not intended to yield realistic predictions for the differential decay rate. Instead, it represents an extreme scenario designed to maximize the difference between the  $K^0$  and  $\overline{K}^0$  energy distributions. In this way, it serves to set an upper bound on the possible size of the experimental asymmetry  $A_3$ .

We use the  $\tau$  rest-frame spectrum shown in Fig. 4 and boost to the laboratory frame to obtain the kaon energy distributions  $S_K(E)$  and  $S_{\overline{K}}(E)$ , following the same strategy used in the computation of  $A_1$  and  $A_2$  asymmetries (see Section VB). Incorporating the detector

efficiency given in Eq. (63), we compute

$$f_3^K(t) = \sum_{i=1}^{10} \int_{\Delta E_i} dE \, S_K(E) F_i(\beta \gamma t) ,$$
 (74)

$$f_3^{\overline{K}}(t) = \sum_{i=1}^{10} \int_{\Delta E_i} dE \, S_{\overline{K}}(E) F_i(\beta \gamma t) . \qquad (75)$$

Using Eq. (62), we obtain an estimate for the experimentally measured asymmetry:

$$A_{Exp,3} \lesssim 9.2 \times 10^{-5} \approx 0.03 \times 2 \text{Re}[\epsilon]$$
 (76)

Within the framework of our simplified spectrum model, this result should be regarded as a rough upper bound. We therefore conclude that the  $A_3$  asymmetry represents a very small effect, below the expected sensitivity of the Belle II experiment.

## D. The total asymmetry

The experimentally observed asymmetry  $A_{Exp,tot}$  at Belle II-type experiment receives contributions from three decays:

$$A_{Exp,tot} = \frac{R_1 A_{Exp,1} + R_2 A_{Exp,2} + R_3 A_{Exp,3}}{R_1 + R_2 + R_3},$$
(77)

where  $R_{1,2,3}$  denote the event fractions of the corresponding decay modes in the total data sample. The decays  $\tau^{\pm} \to K^{\pm}K_S \nu$  and  $\tau^{\pm} \to \pi^{\pm}K_S K_L \nu$  act as backgrounds to the CPasymmetry measurement in  $\tau \to \nu K_S \pi$  decay. Using the results of Eq. (71) and Eq. (76), we find that the following approximations hold to within a few percent accuracy:

$$A_2 = -A_1, A_3 = 0. (78)$$

These simplifications are well justified within the expected experimental precision of Belle II and can therefore be used as working assumptions in the analysis of the measured asymmetry.

#### VI. ADDITIONAL EFFECTS

In this section, we discuss additional effects that may induce artificial contributions to the measured asymmetry, potentially mimicking the genuine CP-violating signal.

#### A. Matter-induced effects in kaon oscillations

The presence of the detector material introduces corrections to the measured CP asymmetry. One possible contribution arises from the different experimental reconstruction efficiencies of particles and antiparticles, which stem from their different interaction probabilities with the detector material. This effect is well established in the literature [19, 20], and leads to a modification of the measured CP asymmetry at the level of  $10^{-3}$ . Within our formalism, this contribution is included in  $A_{Exp,P}^{\text{det}}$ , see Eq. (18) and Eq. (19).

Another effect, specific to neutral kaons, arises from matter-induced modifications of kaon oscillations, as described in Section II C. In the presence of matter, the effective mass eigenstates differ from those in vacuum, as shown in Eq. (31). Consequently, the measured CP asymmetry  $A_{Exp,P}^K$  receives a correction  $A_{Exp,P}^{K,\text{mat}}$  relative to the vacuum case, see Eq. (37). This regeneration effect modifies the effective time evolution of kaons in the detector, thereby shifting the observed CP asymmetry relative to the vacuum expectation. As shown in Eq. (35), this correction depends on the material-dependent kaon regeneration parameter r, defined in Eq. (30), which can be expressed as

$$r = i\pi n L \frac{A - \overline{A}}{p_K} \times \frac{1}{1/2 - i\Delta m \tau_S} \,. \tag{79}$$

Here  $p_K$  is the momentum of the neutral kaon, and  $L = \gamma \beta \tau_S$  is the average decay length of a  $K_S$  in the laboratory frame. In general, r depends on the kaon energy in the laboratory frame, r = r(E). Consequently, the computation of  $A_{Exp,P}^{K,\text{mat}}$  requires averaging over the kaon energy in the laboratory frame, as encoded in the efficiency function (see Eq. (46)),

$$A_{Exp,1}^{K,\text{mat}} = \frac{\int dE \ S_{1,K}(E) \int_0^\infty dt \ F(\beta \gamma t, E) \ \Delta_{\pi\pi}^{\text{mat}}(t, E)}{\int_0^\infty dt \ f_1^K(t) e^{-\Gamma_s t}}$$
(80)

where we define:

$$\Delta_{\pi\pi}^{\text{mat}}(t, E) = -2\text{Re}[r(E)] \left[ e^{-\Gamma_S t} - e^{-\Gamma t} \left( \cos(\Delta m t) + \frac{\text{Im}[r(E)]}{\text{Re}[r(E)]} \sin(\Delta m t) \right) \right]. \tag{81}$$

Eq. (80) and Eq. (81) are valid under the assumption that the entire decay length of the neutral kaon lies within a material characterized with a single regeneration parameter r. Eq. (80) can thus be viewed as a useful approximation, with r computed as an average over different detector components. A fully realistic treatment requires solving the kaon equations of motion in the layered detector environment, see, e.g., [6].

As shown in Eq. (79), the parameter r depends on the kaons regeneration amplitudes  $\Delta \mathcal{A} = \mathcal{A} - \overline{\mathcal{A}}$ . Experimental measurements of  $\Delta \mathcal{A}$  have been performed for different materials in the momentum range  $p_K \in [20, 140] \text{GeV}$  [7], leading to the empirical relation:

$$\left| \frac{\Delta \mathcal{A}}{p_K} \right| = \frac{2.23 \cdot A^{0.758}}{(p_K[\text{GeV}])^{0.614}} ,$$
 (82)

where A denotes the nuclear mass number of the material. The corresponding phase  $\arg(\Delta A)$  was measured for Carbon in the range  $p_K \in [35, 125] \text{ GeV } [14]$ , and found to be consistent with the Regge theory prediction:

$$\arg(\Delta A) \approx -\frac{\pi}{2}(2 - 0.614) = -124.7^{\circ}.$$
 (83)

These measurements, however, are obtained at kaon momenta much higher than those relevant for Belle II, where  $E \sim \mathcal{O}(1\text{GeV})$ . At low energies, theoretical estimates of regeneration amplitudes have been presented in Ref. [8, 13], and measurements exist for Carbon in the range  $p_K \in [250, 750] \,\text{MeV}$  [9]. These results indicate a sizable theoretical uncertainty in the determination of  $\arg(\Delta \mathcal{A})$ , with deviations from the Regge expectation in Eq.(83) of an average of 35° and up to 45°. Such deviations directly affect the determination of r, and consequently of  $A_{Exp,1}^{K,\text{mat}}$ , potentially even changing the sign of the matter-induced correction for a given |r|.

In Fig. 5, we present a theoretical estimate of  $A_{Exp,1}^{K,\text{mat}}$ , computed as a function of |r|, for different values of the theoretically uncertain phase  $\arg(\Delta A)$ . The calculation employs the Belle II efficiency function, as described in Section V, and assumes, for simplicity, that r is independent of the kaon energy.

In Ref. [10], a theoretical estimate of |r| was obtained for different types of detectors by averaging over their various components. For Belle II, this gives  $|r_{\text{Belle II}}| \sim 10^{-3}$ , which corresponds to a correction to the CP asymmetry of

$$\left| A_{Exp,1}^{K,\text{mat}} \right|_{\text{Belle II}} \sim 0.2 \times (2\text{Re}[\epsilon]) \ .$$
 (84)

The uncertainty on this estimate is, however, very large and difficult to quantify reliably.

Because in realistic detectors r is of the same order as  $\epsilon$ , a precise determination of r and its energy dependence is essential for accurate theoretical predictions of the measured CP asymmetry. Moreover, since the effect is energy dependent, it may induce different apparent asymmetries for different decay modes.

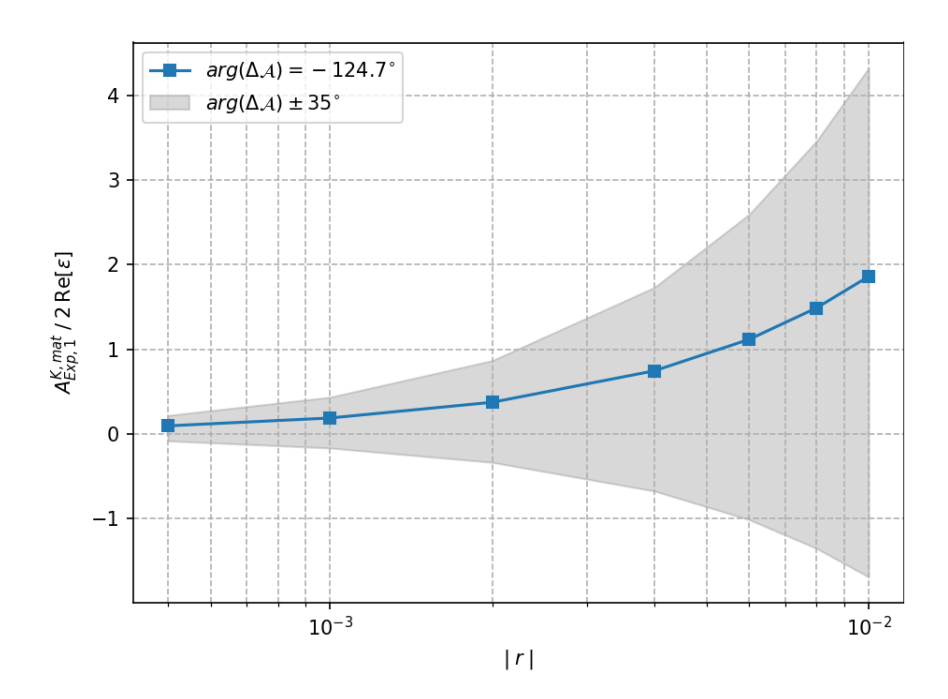


FIG. 5: The correction  $A_{Exp,1}^{K,\mathrm{mat}}$ , Eq. (80), plotted as a function of the magnitude of the kaon regeneration parameter |r|. The calculation assumes |r| to be energy independent and employs the experimental efficiency function of a Belle II obtained in Section V. The solid line corresponds to the phase predicted by Regge theory, see Eq. (83), while the shaded band reflects a theoretical uncertainty of 35 ° on  $\arg(\Delta A)$ .

# B. Forward-backward asymmetry

Another contribution to  $A_{Exp,P}^{\text{det}}$  arises in asymmetric machines, such as the SuperKEKB  $e^+e^-$  collider, where Belle II operates. We discuss this effect for  $A_1$ . The generalization to other processes is straightforward.

The efficiency function  $f_P^{\alpha}(t)$  depends on the energy spectrum of the kaon in the laboratory frame, see Eq. (45). In general, the laboratory-frame energy distribution of a  $K^0$  produced by a  $\tau^+$ ,  $S_{1,K}^+(E)$ , differs from that of a  $\overline{K}^0$  produced by a  $\tau^-$ ,  $S_{1,\overline{K}}^-(E)$ . This difference arises because the  $\tau$  leptons are produced via  $e^+e^- \to \tau^+\tau^-$  processes, and the forward-backward (FB) asymmetry in the 2-to-2 scattering [21] leads to different angular distributions for the  $\tau^+$  and  $\tau^-$  in the center of mass frame, and a different energy spectra in the laboratory frame. Consequently, the resulting efficiency functions differ,  $\Delta f_1^K \neq 0$ , see Eqs.(9) and (45). This effect gives a small correction to the measured asymmetry, see Eq. (18). To estimate

this effect for Belle II, we consider the  $\tau^+\tau^-$  production differential cross section [21],

$$\frac{d\sigma_{ee \to \tau\tau}}{d\cos\theta} \propto F_1(1 + \cos^2\theta) + 2F_2\cos\theta,\tag{85}$$

where  $\theta$  is the scattering angle in the laboratory frame. The FB asymmetry is given by  $A_{FB} = 3F_2/4F_1$ . The leading-order asymmetry can be computed from a one-loop calculation of the 2-to-2 scattering, which is beyond the scope of this work. Here, we assume  $A_{FB} = 1\%$  [21, 22], and use the Belle II-like experimental efficiency and kaon spectrum from Section V. Using Eq. (18), the resulting contribution of the FB asymmetry to the experimental asymmetry is

$$A_{Exp,1}^{\text{det, FB}} \sim 10^{-3} \times (2\text{Re}[\epsilon]) ,$$
 (86)

which is very small compared to the sensitivity of current experiments.

#### VII. CONCLUSION

In the SM, CP violation in  $\tau \to \pi K_S \nu$  decays arises from neutral kaon oscillations in the final state. This CP violation has been studied by the BaBar and Belle collaborations, with the BaBar measurement showing a slight tension with the SM prediction. The Belle II collaboration aims to provide a more precise measurement of this CP asymmetry. In this work, we present a method to predict the experimentally measured CP asymmetry in  $\tau$  decays into final states containing neutral kaons.

We note that the theoretical framework presented here is more general. It can be applied to any decay into a final state containing neutral kaons, such as charm decays  $D^+ \to K_S \pi^+$ . Below, we summarize the main results of this work:

- 1. Theoretical predictions for the CP asymmetries require knowledge of the experimental reconstruction efficiency,  $f_P^{\alpha}(t)$ , as a function of the kaon decay time in the kaon rest frame. In section III, we show that the efficiency function has two contributions, see Eq. (45): (i) the kaon energy distribution in the laboratory frame, which depends on the specific production process P, and (ii) a universal reconstruction efficiency function that depends on the features of the detector and the experiment.
- 2. In section IV, we show that because the reconstruction efficiency depends on the kaons energy spectrum, the decay channel into two neutral kaons,  $\tau \to \nu K_L K_S \pi$ , exhibits

CP violation, see Eq. (62). This arises from the fact that the two neutral kaons are produced with different energy distribution in  $\tau$  decays.

- 3. In section V, we provide a theoretical prediction for the measured CP asymmetries for the processes  $A_1$ ,  $A_2$  and  $A_3$  in a Belle II-like experiment. We find that, within a few percent, it is justified to approximate  $A_2 \approx -A_1$  and  $A_3 \approx 0$ .
- 4. In section VI, we find that matter effects on neutral kaons oscillations can produce a significant correction, up to order  $\mathcal{O}(1)$ , to the measured CP asymmetry, see Eq. (80) and Fig. 5. Further studies and measurements are required to provide a precise theoretical prediction of this correction.

We conclude with the hope that our results will be useful for the upcoming experimental analyses of CP-violating effects in final states with neutral kaons.

#### **ACKNOWLEDGMENTS**

YG is supported in part by the NSF grant PHY-2309456. PL, AM and AR are supported by the German Ministry of Education and Research (BMBF), and the Helmholtz Association (HGF).

#### Appendix A: Kaons energy spectrum in the $\tau$ frame

In this appendix we discuss the simplified theoretical models used to compute  $S_{\alpha,P}^{(\tau)}$ , the energy spectrum of the kaon emitted in the  $\tau$  frame for the processes considered.

 $\tau$  decay into two mesons: We consider the decay process  $\tau^+ \to \overline{\nu} M^+ K_S$ , where the meson  $M^+ = \pi^+$ ,  $K^+$  for  $A_1$  and  $A_2$ , respectively. To describe the decay, we use a simplified model of a point-like interaction between real scalar fields,

$$\mathcal{H}_{int} = g \,\overline{\tau}(x)\nu(x)M^{+}(x)K(x),\tag{A1}$$

where g is a coupling constant, and  $K(x) = K^0(x)$  for process  $A_1$ , and  $K(x) = \overline{K}^0(x)$  for process  $A_2$ . In this simplified model, the scattering matrix element  $\mathcal{M} = \langle M^+ K^0 \overline{\nu} | \mathcal{H}_{int} | \tau^+ \rangle$  is constant,  $\mathcal{M} = g$ . The normalized kaon energy spectrum is obtained from the normalized differential rate as a function of the kaon energy. Since the scattering matrix element is

constant, the kaon's energy distribution essentially depends only on the phase space factor in the differential rate.

 $\tau$  decay into three mesons: We consider the decay of  $\tau$  into three pseudo-scalar mesons  $\tau^+ \to \overline{\nu} \pi^+ K^0 \overline{K}^0$ . To compute the kaons spectrum, we use a simplified model of a four-body decay interaction between real scalar fields, including the propagator of an intermediate  $K^*$  resonance [16, 17]. The interaction is given by

$$\mathcal{H}_{int} = g_1 \, \overline{\tau}(x) \nu(x) \overline{K}^0(x) K^{*+}(x) + g_2 \, K^{*+}(x) \pi^+(x) K^0(x) \tag{A2}$$

The differential decay rate is obtained by treating the  $K^*$  as an intermediate resonance:

$$\mathcal{M} = \frac{g_1 g_2}{q^2 - m_{K^*}^2 + i m_{K^*} \Gamma_{K^*}}.$$
 (A3)

The spectra for  $K^0$  and  $\overline{K}^0$  are defined as the normalized differential rates  $\frac{d\Gamma}{dE_K}$  and  $\frac{d\Gamma}{dE_{\overline{K}}}$ .

- [1] I. Bigi and A. Sanda, Physics Letters B **625**, 47 (2005), arXiv:/hep-ph/0506037.
- [2] Y. Grossman and Y. Nir, JHEP **2012**, 2, arXiv:1110.3790 [hep-ph].
- [3] J. P. Lees et al. (BABAR Collaboration), Phys. Rev. D 85, 031102 (2012).
- [4] M. Bischofberger et al. (Belle Collaboration), Phys. Rev. Lett. 107, 131801 (2011).
- [5] E. Kou et al., Progress of Theoretical and Experimental Physics 2019, 123C01 (2019).
- [6] W. Fetscher, P. Kokkas, P. Pavlopoulos, T. Ruf, and T. Schietinger, Zeitschrift für Physik C: Particles and Fields **72**, 543 (1996).
- [7] A. Gsponer, J. Hoffnagle, W. R. Molzon, J. Roehrig, V. L. Telegdi, B. Winstein, S. H. Aronson, G. J. Bock, D. Hedin, and G. B. Thomson, Phys. Rev. Lett. 42, 13 (1979).
- [8] B. R. Ko, E. Won, B. Golob, and P. Pakhlov, Phys. Rev. D 84, 111501 (2011).
- [9] A. Angelopoulos *et al.*, Physics Letters B **413**, 422 (1997).
- [10] M. Bjørn and S. Malde, JHEP **07**, 106.
- [11] R. A. Briere and B. Winstein, Phys. Rev. Lett. **75**, 402 (1995).
- [12] H. R. Quinn, T. Schietinger, J. a. P. Silva, and A. E. Snyder, Phys. Rev. Lett. 85, 5284 (2000).
- [13] P. H. Eberhard and F. Uchiyama, Nuclear Instruments and Methods in Physics Research Section A: Accelerators, Spectrometers, Detectors and Associated Equipment **350**, 144 (1994).
- [14] J. Roehrig, A. Gsponer, W. R. Molzon, E. I. Rosenberg, V. L. Telegdi, B. D. Winstein, H. G. E.

- Kobrak, R. E. Pitt, R. A. Swanson, S. H. Aronson, and G. J. Bock, *Phys. Rev. Lett.* **38**, 1116 (1977).
- [15] Y. Grossman, Y. Nir, and G. Perez, Phys. Rev. Lett. 103, 071602 (2009).
- [16] R. Decker, E. Mirkes, R. Sauer, and Z. Was, Zeitschrift für Physik C Particles and Fields 58, 445 (1993).
- [17] M. Finkemeier and E. Mirkes, JHEP arXiv:9503474 [hep-ph].
- [18] J. H. Kühn and E. Mirkes, Zeitschrift für Physik C Particles and Fields 56, 661 (1992).
- [19] I. Adachi et al. (Belle II Collaboration), Phys. Rev. D 109, 012001 (2024).
- [20] Belle II Collaboration, *Measurement of Instrumental Asymmetries of Kaons and Pions*, Tech. Rep. BELLE2-NOTE-PL-2022-004 (Belle II Collaboration, 2022) belle II Internal Note.
- [21] T. Ferber and B. Schwartz (Belle, Belle-II), J. Univ. Sci. Tech. China 46, 476 (2016).
- [22] R. Sobie, Nuclear Physics B Proceedings Supplements 76, 75 (1999), tau Lepton Physics.
- [23] G. Calderón, D. Delepine, and G. L. Castro, Phys. Rev. D 75, 076001 (2007).
- [24] D. A. López Aguilar, J. Rendón, and P. Roig, Journal of High Energy Physics 2025, 105 (2025).
- [25] I. Bigi, Nuclear Physics B Proceedings Supplements **253-255**, 91 (2014), the Twelfth International Workshop on Tau-Lepton Physics (TAU2012).
- [26] F.-Z. Chen and X.-Q. Li, International Journal of Modern Physics A 39, 2442010 (2024), https://doi.org/10.1142/S0217751X24420107.
- [27] Y.-F. Shen, W.-J. Song, and Q. Qin, Phys. Rev. D 110, L031301 (2024).
- [28] V. Cirigliano, D. Díaz-Calderón, A. Falkowski, M. González-Alonso, and A. Rodríguez-Sánchez, Journal of High Energy Physics 2022, 152 (2022).
- [29] F.-Z. Chen, X.-Q. Li, S.-C. Peng, Y.-D. Yang, and H.-H. Zhang, Journal of High Energy Physics 2022, 108 (2022).
- [30] P. Pakhlov and V. Popov, Journal of High Energy Physics 2021, 92 (2021).
- [31] F.-Z. Chen, X.-Q. Li, Y.-D. Yang, and X. Zhang, Phys. Rev. D 100, 113006 (2019).
- [32] M. H. V. on behalf of the Belle II collaboration, SciPost Phys. Proc., 003 (2019).
- [33] D. Wang, P.-F. Guo, W.-H. Long, and F.-S. Yu, Journal of High Energy Physics 2018, 66 (2018).
- [34] D. Wang, F.-S. Yu, and H.-n. Li, Phys. Rev. Lett. **119**, 181802 (2017).
- [35] U. Nierste and S. Schacht, Phys. Rev. D 92, 054036 (2015).

- [36] Y. Grossman and M. Savastio, Journal of High Energy Physics 2014, 8 (2014).
- [37] A. Pich, Progress in Particle and Nuclear Physics 75, 41 (2014).
- [38] J. P. Lees et al. (BABAR Collaboration), Phys. Rev. D 87, 052012 (2013).
- [39] B. R. Ko et al. (BELLE Collaboration), Journal of High Energy Physics 2013, 98 (2013).